Late Miocene episodic lakes in the arid Tarim Basin, western China

Weiguo Liu[a,b,1], Zhonghui Liu[c,1], Zhisheng An[a,b], Jimin Sun[d], Hong Chang[a], Ning Wang[a], Jibao Dong[a], and Huanye Wang[a]

[a]State Key Laboratory of Loess and Quaternary Geology, Institute of Earth Environment, Chinese Academy of Sciences, Xi'an 710075, China; [b]School of Human Settlement and Civil Engineering, Xi'an Jiaotong University, Xi'an 710049, China; [c]Department of Earth Sciences, The University of Hong Kong, Hong Kong; and [d]Key Laboratory of Cenozoic Geology and Environment, Institute of Geology and Geophysics, Chinese Academy of Sciences, Beijing 100029, China

The Tibetan Plateau uplift and Cenozoic global cooling are thought to induce enhanced aridification in the Asian interior. Although the onset of Asian desertification is proposed to have started in the earliest Miocene, prevailing desert environment in the Tarim Basin, currently providing much of the Asian eolian dust sources, is only a geologically recent phenomenon. Here we report episodic occurrences of lacustrine environments during the Late Miocene and investigate how the episodic lakes vanished in the basin. Our oxygen isotopic ($\delta^{18}O$) record demonstrates that before the prevailing desert environment, episodic changes frequently alternating between lacustrine and fluvial-eolian environments can be linked to orbital variations. Wetter lacustrine phases generally corresponded to periods of high eccentricity and possibly high obliquity, and vice versa, suggesting a temperature control on the regional moisture level on orbital timescales. Boron isotopic ($\delta^{11}B$) and $\delta^{18}O$ records, together with other geochemical indicators, consistently show that the episodic lakes finally dried up at ~4.9 million years ago (Ma), permanently and irreversibly. Although the episodic occurrences of lakes appear to be linked to orbitally induced global climatic changes, the plateau (Tibetan, Pamir, and Tianshan) uplift was primarily responsible for the final vanishing of the episodic lakes in the Tarim Basin, occurring at a relatively warm, stable climate period.

Tarim Basin | Late Miocene | aridification | tectonic uplift | Milankovitch

Once part of the Neo-Tethys Sea, indicated by the Paleogene littoral-neritic deposits with intercalated marine strata (1), the Tarim Basin in western China (Fig. 1) has experienced dramatic environmental and depositional changes during the Cenozoic. The eventual separation of the basin from the remnant sea probably occurred during the middle to late Eocene (1, 2), and since then, terrestrial sedimentation and environment have prevailed. Today, the basin has relatively flat topography with elevation ranging between 800 and 1,300 m above sea level (asl), surrounded by high mountain ranges with average elevation exceeding 4,000 m. Hyperarid climate prevails with mean annual precipitation <50 mm and evaporation ~3,000 mm. Active sand dunes occupy 80% of the basin, forming the Taklimakan Desert, the largest desert in China and the second largest in the world (3). Thick desert deposits in the basin also provide a major source for dust storms occurring in East Asia (4).

The Tibetan Plateau uplift, long-term global cooling, and the associated retreat of the remnant sea during the Cenozoic, through their complex interplay, may have all contributed to the enhanced aridification in the Asian interior and eventually the desert formation (2, 5–11). Although the onset of Asian desertification is proposed to have started in the earliest Miocene (12, 13), prevailing desert environment in the Tarim Basin, currently providing much of the Asian eolian dust sources (4), is only a geologically recent phenomenon (9). Previous lithological and pollen studies (9, 14, 15) suggest that the currently prevailing desert environment started probably at ~5 Ma. However, what

kind of environmental conditions prevailed before that and how the dramatic changes occurred largely remain elusive.

To better decipher the aridification history, we used a 1,050-m-long, continuous sediment core retrieved from Lop Nor (39°46'0''N, 88°23'19''E) in the eastern basin (Fig. S1). The core site has a relatively low elevation (~800 m asl) (Fig. 1) and thus effectively records basin environment. Previous study sites came from elevated basin margins (9, 14). The core mainly consists of lacustrine sediments with associated fluvial-eolian sands (Fig. 2). The core chronology was established previously based on paleomagnetic polarity (15). The total 706 remanence measurements on the continuous sediment profile allow straightforward correlation with the CK95 geomagnetic polarity timescale (16) and identification of 14 normal (N1–N14) and 13 reversal (R1–R13) polarity zones over the last 7.1 Ma (Fig. S1). The CK95 timescale is largely consistent (within a few ky) with that inferred from marine archives (17) over the last 5.23 Ma, and before 5.23 Ma a practical measure of chronological uncertainty was estimated to be within ~100 ky (18), assuring that the terrestrial records can be directly compared with marine records and orbital changes at the timescale of >100 ky. The derived chronology yields an average sedimentation rate of ~200 m/Ma at lower sections (>1.77 Ma), allowing high-resolution studies of the desertification history at the critical interval.

Boron and oxygen isotopes from carbonates are important environmental indicators (19–25) and used here to infer the environmental evolution in the Tarim Basin. We also present total organic carbon (TOC), calcium carbonate ($CaCO_3$), ostracod, and grain size records to substantiate the isotopic

Significance

The relative roles of the two plausible causes, Cenozoic global cooling and Tibetan Plateau uplift, for the Asian interior aridification/desertification are often difficult to disentangle. High-quality terrestrial records from the Tarim Basin document how enhanced aridification occurred over the last 7 my, from episodic lacustrine environments to the currently prevailing desert environments. During the Late Miocene–Early Pliocene period, episodic occurrences of great lakes and thus wetter climate closely corresponded to periods of high eccentricity and possibly high obliquity, suggesting that the uplifted plateau by then did not effectively block the moisture availability at optimum climatic conditions. The finally irreversible drying up of great lakes at ~4.9 Ma could be attributed to the plateau uplift.
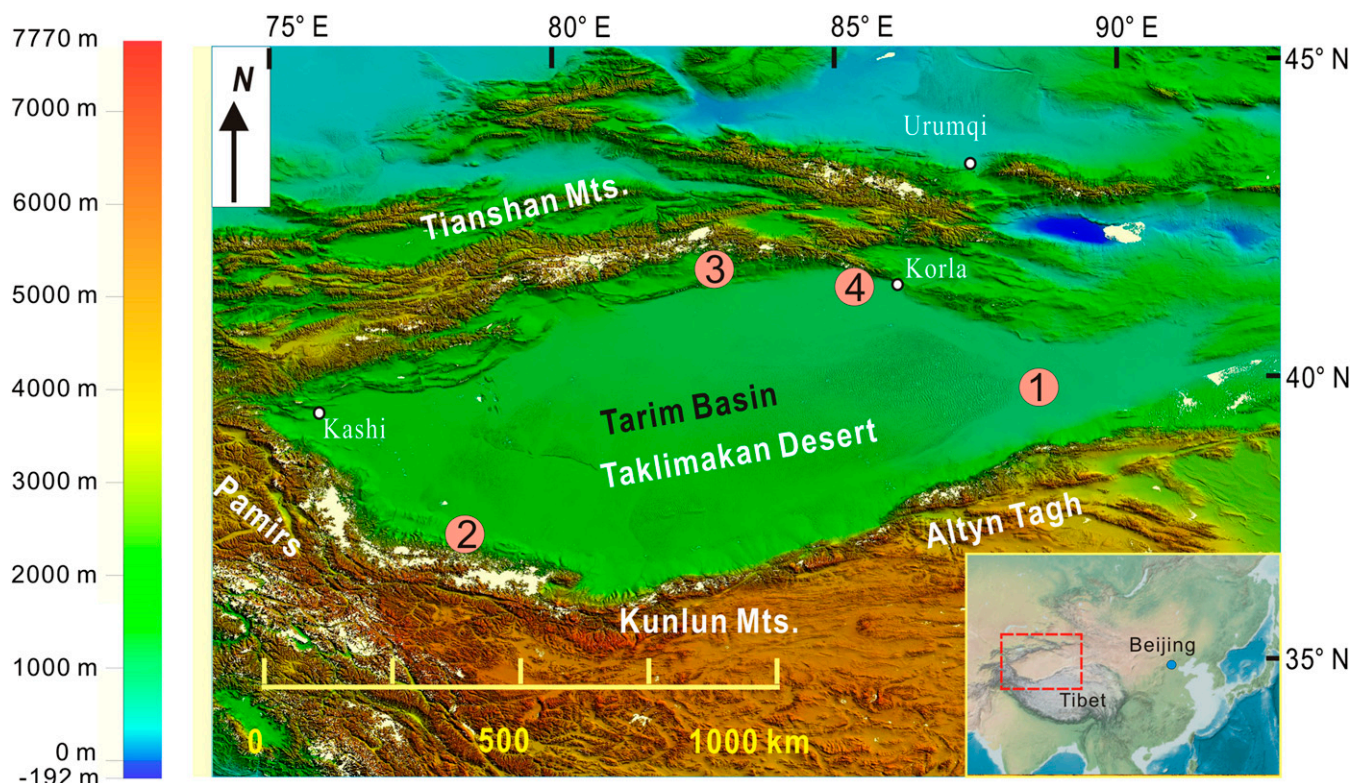
Fig. 1. Digital elevation model of the Tarim Basin and surrounding mountain ranges. The studied 1,050-m sediment core is retrieved from Lop Nor (1), at a relatively low elevation (~800 m asl) in the eastern basin. Also indicated are locations of previous studied sections, near Sanju (2), Kuqa (3), and Korla (4) in the basin.

evidence (*SI Materials and Methods*). Our $\delta^{11}B$ profile shows substantial, stepwise changes over the last ~7.1 Ma (Fig. 2). Carbonate $\delta^{11}B$ values were $-5.0 \pm 1.6‰$ ($n = 3$) before 6.0 Ma, increased rapidly to ~11‰ at 4.9–6.0 Ma, and then stayed at roughly the same level (10.7 ± 2.2‰, $n = 25$) for the remaining 4.9 Ma. Higher-resolution $\delta^{18}O$, TOC, and $CaCO_3$ profiles generally confirm the pattern observed in the low-resolution $\delta^{11}B$ one (Fig. 2). The $\delta^{18}O$ values remained low, ranging from $-10‰$ to $-4‰$ over the last 4.9 Ma. However, $\delta^{18}O$ values frequently oscillated between $-10‰$ and 5‰ before that. Similarly, the TOC profile shows consistently low organic carbon content (0–0.2%) after 4.9 Ma and large fluctuations (0–1.0%) before then. The $CaCO_3$ profile also indicates consistently low values (0–25%) after 4.9 Ma and large fluctuations (0–50%) earlier (Fig. 2).

The multiple proxy records strongly suggest that critical environmental changes must have occurred at ~4.9 Ma. $\delta^{11}B$ values of carbonates from marine sources differ substantially from those of nonmarine carbonates (19–21). $\delta^{11}B$ values after 4.9 Ma are close to those from marine carbonates, but values before 6 Ma fall into the range of lacustrine carbonates (22). Positive $\delta^{18}O$ values before 4.9 Ma also indicate lacustrine environments at that time. Carbonates from modern lakes in arid and semiarid regions of northwestern China show similar positive $\delta^{18}O$ values (23), due to strong evaporation processes. High TOC and $CaCO_3$ contents (Fig. 2) further support that lacustrine environments existed in the basin before ~4.9 Ma. $\delta^{18}O$ values after 4.9 Ma are comparable to those in Cenozoic soil carbonates (24) and ancient marine carbonates in the Tarim Basin (25). However, the accompanying carbonate $\delta^{13}C$ values throughout the record, ranging from $-4‰$ to 1‰ (Dataset S1), are significantly higher than those from Cenozoic soil carbonates reported (26), essentially ruling out the possibility of soil carbonate source. Using modern prevailing desert environment in the basin as an analog, the combined $\delta^{11}B$ and $\delta^{18}O$ evidence thus suggests that

the sediment deposits in the basin after 4.9 Ma must be eolian-fluvial in origin and their sources, at least carbonate grains, came from weathered ancient marine carbonates in nearby regions.

Sedimentological and stratigraphic patterns in other exposed sections from different parts of the basin (9, 14) share great similarity with the Lop Nor core profile (Fig. S1). Episodic lacustrine mudstones and/or siltstones during the Late Miocene were present in all sections and were replaced by fluvial-eolian deposits later. Studies of ostracod assemblages (27) also suggest a shallow paleolake with brackish water environments in the northern basin during the Late Miocene. Changes in the depositional environment from our Lop Nor profile alone could be plausibly explained by a shift in basin center due to tectonic compressions, as evidenced from the slightly uplifted central basin (Fig. 1). However, similar temporal changes occurring basinwide at ~4.9 Ma argue against it. Instead, our results, together with previous studies (5, 14, 15, 27), suggest that paleolakes were widely present in the low lands of the basin during the Late Miocene, much different from currently prevailing desert environments with a few scattered small lakes. The existing evidence, although still limited (Fig. 1), would point to the occurrence of a possible megalake in the Tarim Basin during the Late Miocene.

Three high-resolution records, $\delta^{18}O$, TOC, and $CaCO_3$, further suggest that lacustrine environments before ~4.9 Ma were not permanent (Fig. 2). These large fluctuations indicate frequent switches between lacustrine and fluvial-eolian environments in the basin. High proxy values, $\delta^{18}O$ in particular, appear to indicate lacustrine environments, whereas low values, similar to ones after 4.9 Ma, correspond to fluvial-eolian deposits. This is consistent with lithological features at this interval, showing argillaceous limestone intercalated with clayey layers (15), the occurrence of ostracod assemblages (Fig. 3) from lacustrine sediments, grain size changes (Fig. S2), and detrital carbonate grains identified in photomicrographs of fluvial-eolian deposits (Fig. S3).
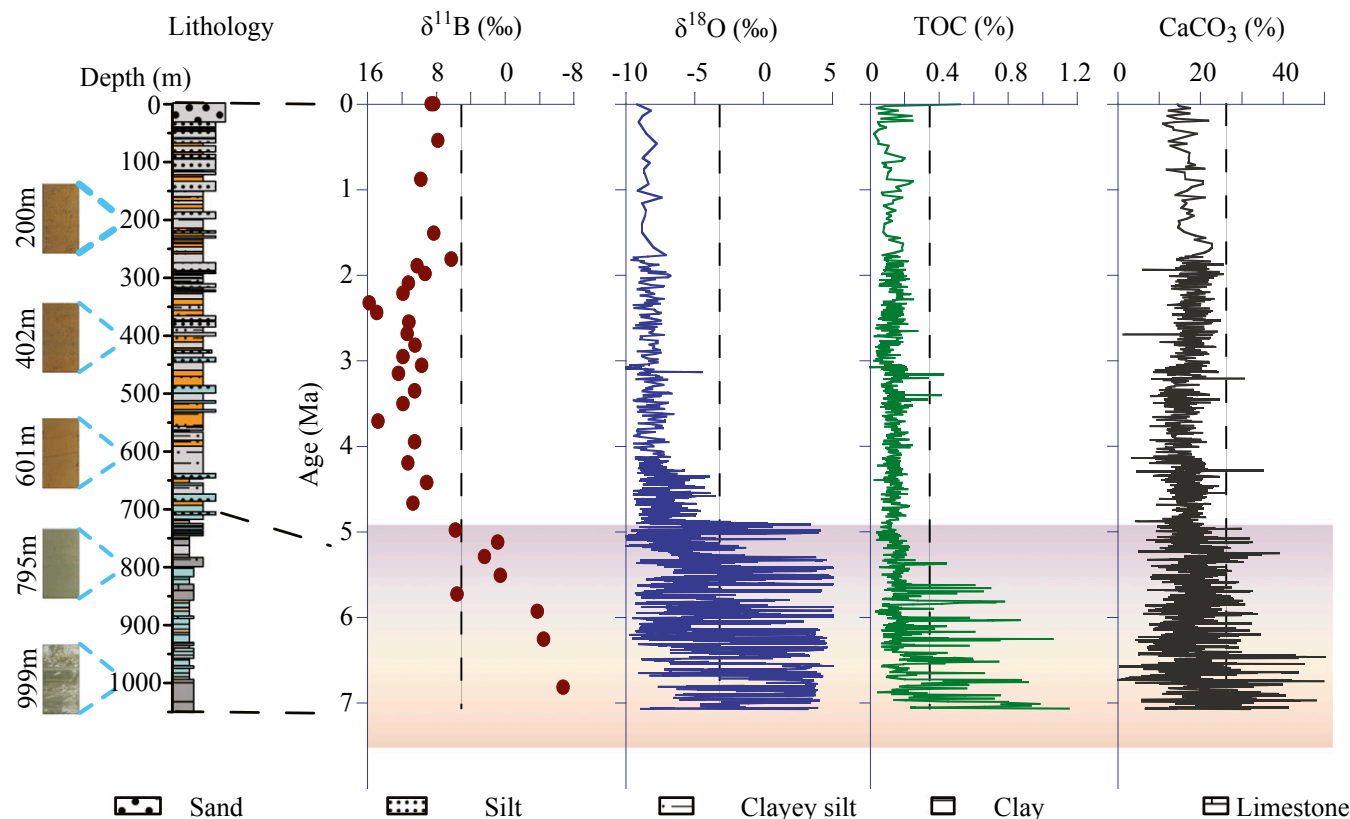
Fig. 2. Records of $\delta^{11}B$, $\delta^{18}O$, TOC, and $CaCO_3$ changes in the Lop Nor profile. Representative photos show lithological changes mainly from lacustrine bluish gray argillaceous limestone to fluvial-eolian brown/red clayey silt, as shown in the lithological column with visual colors indicated (15). High levels and large fluctuations of proxy values occurred only before ~4.9 Ma, and since then, those remain low and within a small range, largely similar to modern conditions. The transition from episodic occurrences of lacustrine phases to prevailing desert environments thus appears to be permanent and irreversible.

To further investigate such episodic changes, we performed spectral analysis on the $\delta^{18}O$ record over the interval 4.5–7.1 Ma. Strong spectral power at orbital frequencies were identified, with periods of ~400 ky throughout the interval, ~41 ky particularly at 6–6.5 Ma, and ~100 ky at 5–6 Ma and 6.5–7.1 Ma (Fig. S4). Precessional ~20-ky power might also have existed but was relatively weak and discontinuous. Lacustrine phase as indicated by high $\delta^{18}O$ values and ostracod assemblages generally occurred at periods of high eccentricity and obliquity (28) (Fig. 3). At 6–6.5 Ma, $\delta^{18}O$ shows clear correspondence to orbital obliquity variation (Fig. 3A). Additionally, the number of low $\delta^{18}O$ values (fluvial-eolian environment) occurred more around 6.5, 6.1, 5.6, and 5.2 Ma, at a ~400-ky beat following orbital eccentricity variation (Fig. 3B). The cluster of high $\delta^{18}O$ values (>0‰) at 4.9–5.0 Ma signals the last occurrence of lacustrine environments in the basin. Our orbital association thus allows us to precisely determine the timing of desert formation at ~4.9 Ma, ~400 ky (an eccentricity cycle) later than the age inferred from basin margins (9, 14) and yet all occurring at eccentricity minima (Fig. 3B). As high eccentricity and obliquity generally correspond to warm conditions at orbital timescales, lacustrine (wet) phase could be associated with warm periods, consistent with the notion that cooler conditions would reduce moisture in the atmosphere and enhance continental drying (10, 11). We recognize that the chronological uncertainty from the geomagnetic polarity timescale before 5.23 Ma, within ~100 ky (18), could confound our association of wet phase with high obliquity, although it is unlikely affected at the 400-ky eccentricity beat. However, the opposite association, wet phase with low obliquity, and the combination with high eccentricity, would require a different, yet

unknown mechanism that is inconsistent with the orbital theory of Pleistocene ice ages.

Superimposed on the orbitally episodic changes, the $\delta^{18}O$ record also shows a long-term trend of deteriorating lacustrine conditions at 4.9–7.1 Ma. As $\delta^{18}O$ values indicate two depositional environments, lacustrine and fluvial-eolian, the range of $\delta^{18}O$ changes (between −10‰ and 5‰) does not vary much over this period (Fig. 3). Rather, the duration of high $\delta^{18}O$ vs. low values would reflect the long-term trend. The mean $\delta^{18}O$ values over 40-ky and 400-ky intervals both show a decreasing trend, with dominant lacustrine phase before 6.1 Ma, more developed fluvial-eolian environment at 5.7–6.1 Ma, a return to slightly better lacustrine environment at 5.3–5.7 Ma, and lacustrine phase permanently vanished around 4.9 Ma (Fig. 4).

The gradual disappearance of the Tarim episodic lakes could be potentially explained by the two driving forces, plateau uplift (the Tibetan Plateau, Pamir Plateau, and Tianshan) and long-term global cooling. However, the long-term global climate was relatively warm and stable during this period (Fig. 4). The global benthic $\delta^{18}O$ record (29) shows that much of the Miocene cooling occurred between 15 and 11 Ma, and the cooling between 8 and 5 Ma was minimal. Supporting this view, sea surface temperature records from the northwestern Pacific (30) show that almost no cooling occurred between 6 and 4 Ma (perhaps further to 3 Ma) (Fig. 4). Particularly, the mean global climate (29, 30) was even warmer at 4.1–4.5 Ma than at 5.7–6.1 Ma, whereas lacustrine phase permanently disappeared after ~4.9 Ma (Fig. 4), indicating decoupling of the lake evolution from global climate. Therefore, long-term global cooling might have played a subordinate role in the lake disappearance.
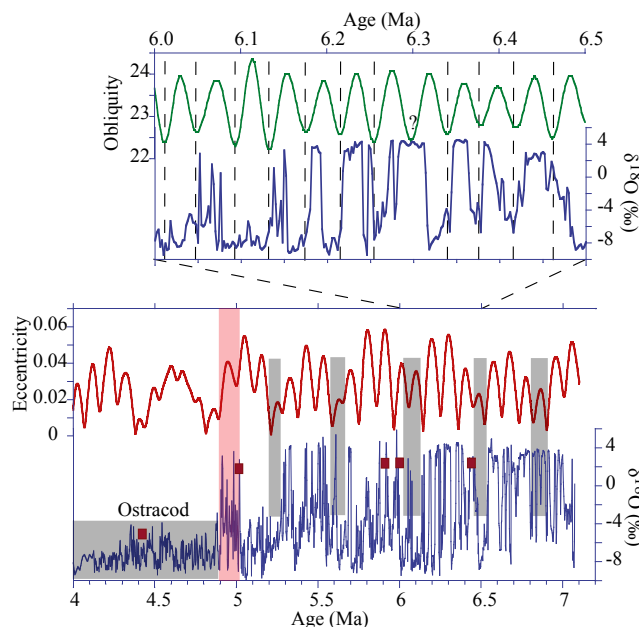
Fig. 3. $\delta^{18}O$ fluctuations linked to eccentricity and obliquity orbital variations at 4.5–7.1 Ma. Lacustrine phases (high $\delta^{18}O$) generally correspond to periods of high eccentricity and obliquity. Fluvial-eolian environment (low $\delta^{18}O$, highlighted with gray bars), developed more around 6.5, 6.1, 5.7, and 5.2 Ma, at a ~400-ky eccentricity beat. The red bar indicates the last occurrence of lacustrine environment at ~4.9 Ma. Occurrences of ostracod assemblages with total number >100 are also indicated.

Instead, the growth of surrounding mountain ranges (Tibetan, Pamir, and Tianshan) may have blocked moisture from the west and south, changed air circulations, and eventually led to the permanent lake disappearance within the basin. Today, the Tarim Basin receives limited moisture from westerlies (31) through the Pamir and Tianshan Ranges (and perhaps from the Indian Ocean in summertime as well). Although the Indo–Eurasian convergence since the Late Eocene resulted in high elevations of the Tibetan Plateau and, to a lesser degree, surrounding mountains including Pamir and Tianshan by the mid-Miocene time (8), tectonic activities in broad areas around the Tarim Basin appear to be rejuvenated since the Late Miocene. Tectonic deformations during the Late Miocene–Early Pliocene inferred from growth strata, sedimentary facies changes, and low-temperature thermochronologic studies occurred in Tianshan to the north of the Tarim Basin, in the Kunlun Mountains to its south and the Pamir to its west (32–35). Syntectonic growth strata from the foreland basins of the Kunlun and Tianshan Ranges (32) show that strong crust shortening and potential mountain uplift initiated ~6.5–5 Ma and lasted to the Early Pleistocene (Fig. S5), similarly reported in northern Pamir (33). Cenozoic sequences in the Pamir–Tianshan convergence zone, changing from an arid continental plain to an intermountain basin by ~5 Ma, support surface uplift of the west margin of the Tarim Basin (34). Occurrence of detrital apatite fission track ages from West Kunlun Ranges (35) also peaked at ~4.5 Ma (Fig. 4). Thus, the reactivated uplift of Pamir and West Kunlun Ranges and northward movement of Pamir during the Late Miocene–Pliocene would progressively block moisture into the basin and enhance regional aridity to a certain threshold to terminate lacustrine environments even during warm periods with favorable orbital configuration. Although inconsistencies indeed exist in linking regional climatic and environmental changes to tectonic events (8), the final vanishing of the Tarim episodic lakes is better explained by tectonic factors.

Therefore, our multiple-proxy results consistently show that the Taklimakan sand sea began to form at ~4.9 Ma and that the

transition into prevailing desert environment was permanent and irreversible. The episodic occurrences of lacustrine environments at favorable climatic conditions (warm periods) during the Late Miocene suggest that uplifted mountain ranges then were not high enough to effectively block moisture from being transported into the basin. The transition from episodic lacustrine environments to prevailing desert deposits was gradual, from 7.1 Ma (or earlier beyond our record) to 4.9 Ma, for which we suggest that although long-term global cooling enhanced the overall aridification in the Asian interior during the Late Cenozoic (10, 11), plateau uplift played a more important role in finally drying up the episodic lakes within a relatively warm, stable climate period, thus decoupling regional climate temporally from a global trend. Our high-resolution records thus demonstrate that regional climate in the Tarim Basin reached a critical state in the Late Miocene, with the dual effects from global climate conditions and regional tectonic settings then. With global climate remaining relatively stable and warm entering the Pliocene, by ~3–4 Ma (Fig. 4), drying up of episodic lakes at ~4.9 Ma could thus be largely attributed to rejuvenated tectonic activities.

Materials and Methods

We conducted 33 $\delta^{11}B$, ~2,000 $\delta^{18}O$ and $CaCO_3$, and ~1,000 TOC analyses from the 1,050-m-long sediment core. High-resolution (2–4 ky) measurements for the last three proxies were performed from the core depth of 300–1,050 m to resolve detailed features at orbital timescales. For $\delta^{11}B$ analysis, about 5 g of clay sediments were dissolved in HCl and purified. The isotope composition of boron was measured using a positive thermal ionization mass spectrometry based on the measurement of $Cs_2BO_2^+$ with graphite and reported in the delta (δ) notation relative to National Institute of Standards and Technology standard NIST SRM951. Typical analytical error is within 0.15‰. For $\delta^{18}O$ analysis, ~1 g of sediments was grounded and sieved through a 100-mesh screen. Analyses of carbonate samples were performed using an isotope ratio mass spectrometer [MAT-252 (Finnigan)] with an automated carbonate preparation device
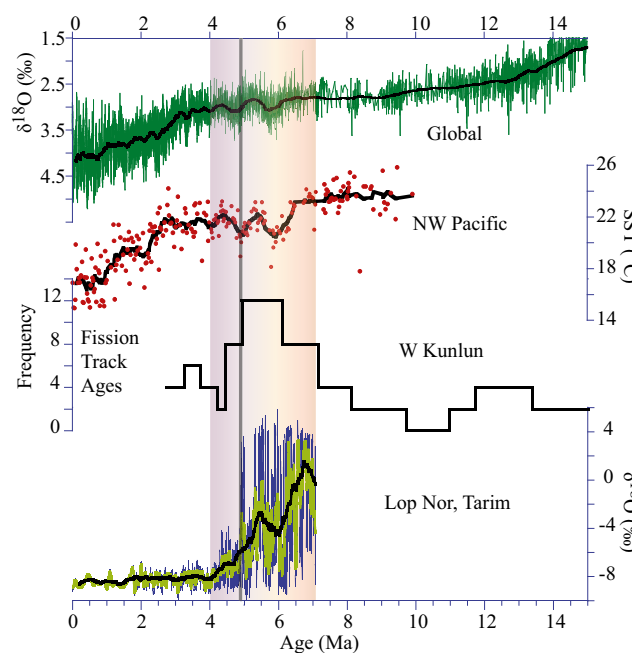

Fig. 4. Long-term $\delta^{18}O$ changes compared with global climatic conditions and regional tectonic activities. Global benthic $\delta^{18}O$ (29) and northwestern Pacific SST (30) records show minimal long-term changes at 4–7 Ma, whereas occurrences of detrital apatite fission track ages (35) in northern western Kunlun peaked, and the Tarim episodic lakes gradually vanished. The dark thick lines are their 400-ky running means, and the light green line on $\delta^{18}O$ represents the 40-ky running mean.

(Kiel II). Oxygen isotope composition is expressed in the delta (δ) notation relative to the V-PDB (Vienna-Pee Dee Belemnite) standard. Typical analytical error is within ±0.1‰. Organic carbon content was determined with the wet oxidation method, and $CaCO_3$ was determined by using the neutralization-titration method. Detailed methods and any associated references can be found in *SI Materials and Methods*.

1. Zhang KX, et al. (2010) Paleogene-Neogene stratigraphic realm and sedimentary sequence of the Qinghai-Tibet Plateau and their response to uplift of the plateau. *Sci China Earth Sci* 53(9):1271–1294.
2. Bosboom RE, et al. (2011) Late Eocene sea retreat from the Tarim Basin (West China) and concomitant Asian paleoenvironmental change. *Palaeogeogr Palaeoclimatol Palaeoecol* 299(3-4):385–398.
3. Zhu ZD, Wu Z, Liu S, Di XM (1980) *An Outline on Chinese Deserts* (Science Press, Beijing), pp 1–107.
4. Zhang XY, et al. (2003) Sources of Asian dust and role of climate change versus dersitification in Asian dust emission. *Geophys Res Lett* 30(24):2272.
5. Ruddiman WF, Kutzbach JE (1989) Forcing of the late Cenozoic northern hemisphere climate by plateau uplift in the Southern Asia and American West. *J Geophys Res* 94(D15):18409–18427.
6. Harrison TM, Copeland P, Kidd WS, Yin A (1992) Raising Tibet. *Science* 255(5052):1663–1670.
7. An Z, Kutzbach JE, Prell WL, Porter SC (2001) Evolution of Asian monsoons and phased uplift of the Himalaya-Tibetan plateau since Late Miocene times. *Nature* 411(6833):62–66.
8. Molnar P (2005) Mio-Pliocene growth of the Tibetan Plateau and evolution of East Asian climate. *Palaeontol Electronica* 8(1):2A.
9. Sun J, Liu T (2006) The age of the Taklimakan Desert. *Science* 312(5780):1621.
10. Tang ZH, et al. (2011) Late Cenozoic central Asian drying inferred from a palynological record from the northern Tian Shan. *Earth Planet Sci Lett* 302(3-4):439–447.
11. Miao Y, Herrmann M, Wu F, Yan X, Yang S (2012) What controlled Mid–Late Miocene long-term aridification in Central Asia? — Global cooling or Tibetan Plateau uplift: A review. *Earth Sci Rev* 112(3-4):155–172.
12. Guo ZT, et al. (2002) Onset of Asian desertification by 22 Myr ago inferred from loess deposits in China. *Nature* 416(6877):159–163.
13. Qiang XK, et al. (2011) New eolian red clay sequence on the western Chinese Loess Plateau linked to onset of Asian desertification about 25 Ma ago. *Sci China Earth Sci* 54(1):136–144.
14. Zhang ZQ, Sun JM (2011) Palynological evidence for Neogene environmental change in the foreland basin of the southern Tianshan range, northwestern China. *Global Planet Change* 75(1-2):56–66.
15. Chang H, et al. (2012) Magnetostratigraphic and paleoenvironmental records for a Late Cenozoic sedimentary sequence drilled from Lop Nor in the eastern Tarim Basin. *Global Planet Change* 80-81:113–122.
16. Cande SC, Kent DV (1995) Revised calibration of the Geomagnetic Polarity Time Scale for the Late Cretaceous and Cenozoic. *J Geophys Res* 100(B4):6093–6095.
17. Lisiecki LE, Raymo ME (2005) A Pliocene-Pleistocene stack of 57 globally distributed benthic $\delta^{18}O$ records. *Paleoceanography* 20(1):PA1003.
18. Kent DV (1999) Orbital tuning of geomagnetic polarity time-scales. *Philos Trans R Soc Lond A* 357(1757):1995–2007.
19. Barth S (1993) Boron isotope variations in nature: A synthesis. *Geol Rundsch* 82(4):640–651.
20. Slack JF, Palmer MR, Stevens BPJ (1989) Boron isotope evidence for the involvement of non-marine evaporites in the origin of the Broken Hill ore deposits. *Nature* 342(6252):913–916.
21. Moldovanyi EP, Walter LM, Land LS (1993) Strontium, boron, oxygen, and hydrogen isotope geochemistry of brines from basal strata of the Gulf Coast sedimentary basin, USA. *Geochim Cosmochim Acta* 57(9):2083–2099.
22. Xiao YK, Sun DP, Wang YH, Qi HP, Jin L (1992) Boron isotopic compositions of brine, sediments, and source water in Da Qaidam Lake, Qinghai, China. *Geochim Cosmochim Acta* 56(4):1561–1568.
23. Liu W, Li X, Zhang L, An Z, Xu L (2009) Evaluation of oxygen isotopes in carbonate as an indicator of lake evolution in arid areas: The modern Qinghai Lake, Qinghai-Tibet Plateau. *Chem Geol* 268(1-2):126–136.
24. Kent-Corson ML, et al. (2009) Stable isotopic constraints on the tectonic, topographic, and climatic evolution of the northern margin of the Tibetan Plateau. *Earth Planet Sci Lett* 282(1-4):158–166.
25. Gao QD (2011) C, O, Sr isotope composition of the carbonate in Ordovician in Tarim Basin and implication on fluid origin. *J Zhejiang Univ* 38(5):579–583.
26. Rowley DB, Currie BS (2006) Palaeo-altimetry of the late Eocene to Miocene Lunpola basin, central Tibet. *Nature* 439(7077):677–681.
27. Sun ZC, et al. (1999) Cenozoic Ostracoda and palaeoenvironments of the northeastern Tarim Basin, western China. *Palaeogeogr Palaeoclimatol Palaeoecol* 148(1-3):37–50.
28. Laskar J, et al. (2004) A long term numerical solution for the insolation quantities of the Earth. *Astron Astrophys* 428(1):261–285.
29. Zachos J, Pagani M, Sloan L, Thomas E, Billups K (2001) Trends, rhythms, and aberrations in global climate 65 Ma to present. *Science* 292(5517):686–693.
30. LaRiviere JP, et al. (2012) Late Miocene decoupling of oceanic warmth and atmospheric carbon dioxide forcing. *Nature* 486(7401):97–100.
31. Aizen VB, et al. (2006) Climatic and atmospheric circulation pattern variability from ice-core isotope/geochemistry records (Altai, Tien Shan and Tibet). *Ann Glaciol* 43(1):49–60.
32. Sun JM, Li Y, Zhang ZQ, Fu BH (2009) Magnetostratigraphic data on the Neogene growth folding in the foreland basin of the southern Tianshan Mountains. *Geology* 37(11):1051–1054.
33. Coutand I, et al. (2002) Late Cenozoic tectonic development of the intramontane Alai Valley, (Pamir-Tien Shan region, central Asia): An example of intracontinental deformation due to the Indo-Eurasia collision. *Tectonics* 21(6):1053.
34. Wang X, et al. (2014) Cenozoic paleo-environmental evolution of the Pamir-Tien Shan convergence zone. *J Asian Earth Sci* 80:84–100.
35. Wang GC, et al. (2011) Spatio-temporal framework of tectonic uplift stages of the Tibetan Plateau in Cenozoic. *Sci China Earth Sci* 54(1):29–44.